Laboratory Investigation (2021) 101:155–164
https://doi.org/10.1038/s41374-020-00496-z

ARTICLE

MicroRNA-130b functions as an oncogene and is a predictive marker of poor prognosis in lung adenocarcinoma

Yeseul Kim[1] · Hyunsung Kim[2] · Seongsik Bang[2] · Seungyun Jee[2] · Kiseok Jang[2]

Received: 29 June 2020 / Revised: 17 September 2020 / Accepted: 18 September 2020 / Published online: 30 September 2020

Abstract

Lung cancer is an aggressive disease and the leading cause of cancer-related deaths worldwide. In the past several decades, the incidence of adenocarcinoma has significantly increased, and accounts for ~40% of all lung cancer cases. In the present study, we investigated the clinicopathologic significance of microRNA-130b (miR-130b) in lung adenocarcinoma and analyzed its cancer-specific functions. RNA was extracted from formalin-fixed paraffin-embedded specimens of 146 lung adenocarcinoma cases, and miR-130b expression was analyzed using quantitative real-time polymerase chain reaction. NCI-H1650 cells were transfected with miR-130b mimic and inhibitor to determine its effects on tumor cell proliferation, migration, and invasion. The expression of miR-130b in lung adenocarcinoma tissues was classified into two groups according to the median value. High expression of miR-130b was associated with higher histological grade, advanced pathologic T stage, lymph node metastasis, and lymphovascular invasion. Moreover, survival analysis showed that high miR-130b expression was significantly associated with unfavorable prognosis. In addition, miR-130b upregulation promoted cell migration and invasion, while its downregulation resulted in decreased cell proliferation, migration, and wound healing in in vitro experiments. In conclusion, these findings suggest that miR-130b promotes tumor progression and serves as a biomarker of poor prognosis for patients with lung adenocarcinoma. Hence, targeting miR-130b may serve as a potential therapeutic strategy for lung cancer.

Introduction

Lung cancer is one of the leading causes of cancer deaths worldwide [1]. Over the past decade, the treatment modalities for lung cancer have evolved [2]. The use of tyrosine kinase inhibitors targeting epidermal growth factor receptor, anaplastic lymphoma kinase, and ROS1 and immune checkpoint inhibitors blocking programmed cell death protein 1/programmed death-ligand 1 interaction has drastically changed the treatment paradigms for patients with non-small cell lung cancer [3]. Although the overall patient outcome has improved significantly due to advances in treatment modalities, the prognosis of lung cancer is still unsatisfactory [1]. This highlights the need for identifying a novel biomarker that can serve as a candidate for targeted therapy and predict patient outcome.

MicroRNAs (miRNAs), a group of short non-coding RNAs (20–25 nucleotides), regulate gene expression at the post-transcriptional level via binding to complimentary sequences in the 3′ untranslated region of their target messenger RNA (mRNA) transcripts [4–6]. Moreover, they suppress the translation or degradation of their target mRNAs by forming RNA-induced silencing complexes [7]. Fundamentally, miRNAs play important roles in various biological processes, such as development, differentiation, proliferation, and apoptosis [8]. In addition, an increasing number of studies have revealed the differential expression of miRNAs in various cancer types, and their effect on cancer-related processes, including tumor cell proliferation, migration, and invasion [9–12]. Furthermore, previous studies revealed that miRNAs are aberrantly expressed in human cancers and play oncogenic or tumor suppressive roles according to the cancer type [6, 13, 14].

These authors contributed equally: Yeseul Kim, Hyunsung Kim

✉ Kiseok Jang
medartisan@hanyang.ac.kr

[1] Department of Pathology, University of Ulsan College of Medicine, Asan Medical Center, Seoul, Republic of Korea

[2] Department of Pathology, Hanyang University College of Medicine, Seoul, Republic of Korea

Among miRNAs, miRNA-130b (miR-130b), located at chromosome 22q11, has been reported to be related to tumorigenesis of various cancers. miR-130b was shown to promote cell migration and invasion in bladder cancer, glioma, esophageal cancer, and Ewing sarcoma [15–18]. In addition, it has been reported that miR-130b suppresses apoptosis in lung cancer and renal cell carcinoma, thus promoting tumor cell proliferation [19, 20]. In colorectal cancer, miR-130b upregulation has been associated with enhanced epithelial–mesenchymal transition and angiogenesis [21]. Moreover, miR-130b contributes to chemoresistance in breast cancer and lung cancer by activating the phosphoinositol 3 kinase/protein kinase B and Wnt/β-catenin pathways [22, 23].

In this study, we analyzed miR-130b expression in human lung adenocarcinoma tissues using quantitative real-time polymerase chain reaction (qRT-PCR) and evaluated its correlation with various clinicopathologic characteristics. Furthermore, we performed in vitro experiments to reveal the role of miR-130b in tumor cell proliferation, migration, and invasion.

Materials and methods

Patients and specimens

Tissue samples were obtained from 184 lung adenocarcinoma patients who underwent curative resection at Hanyang University Hospital from 2003 to 2014. None of the patients received preoperative radiotherapy or chemotherapy. Clinicopathologic data were collected from medical records and histopathological reports. The histopathological diagnoses were made according to the World Health Organization (WHO) classification [24]. Histologic grading was determined based on conventional histological criteria, including architectural abnormality and cytologic atypia. Most cases of histologic grade 1 were lepidic predominant subtype, grade 2 were acinar or papillary predominant subtype, and grade 3 were solid or micropapillary predominant subtype based on the 2015 WHO classification. The disease stage of the cases was assessed according to the 8th edition of the American Joint Committee on Cancer (AJCC) tumor-node-metastasis (TNM) staging system [25]. In this study, histologic grade was dichotomized as low (Grade 1) or high (Grade 2 + Grade 3), pT (pathologic T) stage as early (pTis + pT1) or advanced (pT2–pT4), AJCC stage as early (stage I) or advanced (stage II–IV), and primary tumor size as small (< 3 cm) or large (≥ 3 cm). Disease-free survival (DFS) was measured from the date of surgical resection to the date of recurrence or death owing to lung adenocarcinoma or the date of the last follow-up. Overall survival (OS) was measured from the date of operation until the date of death or last follow-up. This study was approved by the Institutional Review Board of Hanyang University Hospital (IRB file no. HYUH 2016-07-038).

miRNA expression data collection from the Cancer Genome Atlas (TCGA) dataset

Level 3 miRNA expression data and corresponding clinical information for 452 lung adenocarcinoma samples were obtained from TCGA data portal (https://portal.gdc.cancer.gov/). After excluding 12 cases with positive surgical margins and 5 cases with insufficient clinical information, 435 cases were selected.

qRT-PCR

To identify the most representative and non-necrotic tumor area, we reviewed all hematoxylin and eosin-stained slides and marked the most appropriate tumor portion. Three or four 10-μm thick sections from each paraffin block were collected. Total RNA was extracted from the formalin-fixed paraffin-embedded (FFPE) tissues using the miRNeasy FFPE kit (Qiagen, Hilden, Germany) according to the manufacturer's instructions. The human lung adenocarcinoma cell line (NCI-H1650) was purchased from the Korean Cell Line Bank (Seoul, Korea) and RNA was extracted using TRIzol reagent (Thermo Fisher Scientific, Illinois, USA). RNA concentration and purity were measured using the NanoDrop 2000 spectrophotometer (NanoDrop Technologies, Waltham, MA, USA). Universal cDNA synthesis kit (Exiqon, Vedbaek, Denmark) was used to convert RNA into cDNA. qRT-PCR experiments were performed using a mixture of diluted cDNA samples, miR-130b-specific primer sets (Exiqon), and ExiLENT SYBR Green Master mix (Exiqon). qRT-PCR was performed on the CFX96 thermocycler (Bio-Rad, Hercules, CA, USA) under the following conditions: 95 °C for 15 min, followed by 45 cycles of 95 °C for 10 s and 60 °C for 1 min. After PCR amplification, melting curve analysis was performed to confirm the specificity of PCR products. The expression level of miR-130b was calculated relative to the U6 small nuclear RNA using the $2^{-\Delta\Delta Ct}$ method. miR-130b expression was classified into low or high expression according to the median value.

Cell culture and transfection

The human lung adenocarcinoma cell line, NCI-H1650, was obtained from the Korean Cell Line Bank (Seoul, Korea). NCI-H1650 cells were cultured in Roswell Park Memorial Institute-1640 medium containing 10% fetal bovine serum and 1% penicillin (Welgene, Daegu, Korea). All cells were

grown at 37 °C in a humidified atmosphere of 5% CO_2. Penicillin was removed from the medium 48 h before performing any experiment.

miR-130b mimics, miR-130b inhibitor, and control were synthesized by Bioneer (Daejeon, Korea). Cell transfection was performed using Lipofectamine 2000 (Invitrogen, Carlsbad, CA, USA) according to the manufacturer's instructions. The cells were prepared for further analyses after 48 h of transfection.

Cell proliferation assay

To evaluate the effect of miR-130b on cell proliferation, NCI-H1650 cells were transfected with miR-130b mimic and inhibitor. After harvesting, equal numbers of cells were seeded in a six-well plate. Every 24 h, the transfected cells were manually counted for 4 days using trypan blue staining, and each experiment was performed in triplicate.

The MTT assay was performed using the Vybrant MTT Cell Proliferation assay kit (Invitrogen, Carlsbad, CA, USA). At 8 h after transfection, NCI-H1650 cells were seeded in a 96-well culture plate. After 24, 48, and 72 h of incubation, 10 µL of MTT solution was added into each well for 2 h at 38 °C to solubilize the crystals. The optical density was determined with a spectrophotometer at a wavelength of 490 nm.

Transwell migration and invasion assays

Migration and invasion assays were performed using transwell chambers. For the migration assay, 1×10^5 cells were seeded into the upper chamber of the transwell (Corning, NY, USA). For the invasion assay, 1×10^5 cells were seeded in the upper chamber precoated with Matrigel. In both the assays, cell suspension in medium without serum was seeded in the upper chamber, and cells in medium containing 10% fetal bovine serum were seeded in the lower chamber as chemoattractant. After 24 h, cells that did not migrate or invade were removed with a cotton swab. The membranes were then fixed and stained with 0.5% crystal violet. The number of invading and migrating cells in three random fields were counted using a light microscope, and each experiment was repeated in triplicate.

Wound-healing assay

The transfected cells were cultured in serum-free Roswell Park Memorial Institute-1640 medium and seeded in culture inserts, which artificially produced homogenous wounds covered with sterile silicone insert. After taking off the insert, cells were gently washed twice with Dulbecco's phosphate-buffered saline to remove any free-floating cells or debris, and the medium was replaced with medium containing 10% fetal bovine serum. The cells were incubated at 37 °C for 24 h. The wounds covered by proliferating cells were observed under a phase-contrast microscope after 24 and 48 h. All experiments were performed in triplicate.

Statistical analysis

Statistical analysis was performed using SPSS 21.0 software (SPSS, Chicago, IL, USA). $\chi 2$ test and Mann–Whitney U test was used to evaluate the association between miR-130b expression and various clinicopathologic features of lung adenocarcinoma. Both DFS and OS were measured from the day of surgery and their curves were generated using Kaplan–Meier analysis, and the log-rank test was applied to establish the level of significance. A Cox proportional hazard regression model was employed for both univariate and multivariate survival analyses. Student's t test was used for comparing the means of two groups. A p value of <0.05 was considered as statistically significant.

Results

Clinical and pathologic characteristics of the cohort

The clinicopathologic parameters assessed included age, sex, primary tumor size, histologic grade, pT stage, AJCC stage, lymph node metastasis, pleural invasion, lymphovascular invasion, and perineural invasion (Table 1). Among 184 cases, 38 cases with unavailable paraffin tissues or failed RNA extraction were excluded. The miRNA expression data of 146 cases were collected. Approximately two-thirds of the patients were older than 60 years of age ($n = 90$, 61.6%), and the percentage of females was slightly higher than that of males ($n = 83$, 56.8%). In addition, more than half the cases exhibited small tumor size ($n = 94$, 64.4%), high histologic grade (grade 2 and grade 3; $n = 119$, 81.5%), and early AJCC stage ($n = 90$, 61.7%).

Correlation between miR-130b expression and clinicopathologic parameters in lung adenocarcinoma

We next analyzed the correlation between miR-130b expression and clinicopathologic parameters, including age, sex, primary tumor size, histologic grade, pT stage, AJCC stage, lymph node metastasis, and pleural invasion (Table 2). Results showed that high miR-130b expression was associated with aggressive phenotypes, such as higher histologic grade ($p < 0.001$), advanced T stage ($p = 0.012$), advanced AJCC stage ($p = 0.004$), lymph node metastasis ($p = 0.021$), and lymphovascular invasion ($p = 0.030$); however, no

Table 1 Clinical and pathologic characteristics of patients with lung adenocarcinoma.

	Number of patients	
	Total ($n = 146$)	%
Age		
<60 years	56	38.4
≥60 years	90	61.6
Sex		
Male	63	43.2
Female	83	56.8
Primary tumor size		
<3 cm	94	64.4
≥3 cm	52	35.6
Histologic grade		
G1	27	18.5
G2	103	70.5
G3	16	11.0
Pathologic T category		
Tis	2	1.4
T1	64	43.8
T2	70	47.9
T3	6	4.1
T4	4	2.7
AJCC stage		
0	2	1.4
I	88	60.3
II	29	19.9
III	27	18.5
Pathologic N category		
N0	104	71.2
N1	20	13.7
N2	20	13.7
N3	2	1.4
Pleural invasion		
PL0	91	62.3
PL1	44	30.1
PL2	10	6.8
PL3	1	0.7
Lymphovascular invasion		
Absent	88	60.3
Present	58	39.7
Perineural invasion		
Absent	117	80.1
Present	29	19.9

AJCC American Joint Committee on Cancer.

statistically significant correlation was observed with age, sex, primary tumor size, pleural invasion, or perineural invasion. Additionally, we compared the mean expression level of miR-130b in each clinicopathologic parameters by Mann–Whitney *U* test. Results showed that mean miR-130b expression was also associated with aggressive phenotypes, such as higher histologic grade ($p = 0.002$), advanced AJCC stage ($p = 0.013$), and lymph node metastasis ($p = 0.042$).

Prognostic value of miR-130b expression in lung adenocarcinoma

The median DFS and OS for all patients were 37.6 and 47.6 months, respectively. Patients with low miR-130b expression showed significant DFS prolongation compared to those with high miR-130b expression ($p < 0.001$; Fig. 1a). The OS rate of patients with low miR-130b expression was also higher than that of patients with high miR-130b expression ($p < 0.001$; Fig. 1b).

The results of univariate survival analysis are shown in Table 3. Larger primary tumor size ($p = 0.005$), higher histologic grade ($p = 0.007$), advanced pT stage ($p = 0.013$), advanced AJCC stage ($p < 0.001$), lymph node metastasis ($p < 0.001$), lymphovascular invasion ($p < 0.001$), perineural invasion ($p = 0.013$), and high miRNA-130b expression ($p < 0.001$) were predictors of poor DFS. In addition, larger primary tumor size ($p = 0.008$), higher histologic grade ($p = 0.020$), advanced pT stage ($p = 0.007$), advanced AJCC stage ($p < 0.001$), lymph node metastasis ($p < 0.001$), pleural invasion ($p = 0.012$), lymphovascular invasion ($p = 0.001$), and high miRNA-130b expression ($p = 0.001$) were also predictors of poor OS. In multivariate Cox regression analysis, the parameters that were not significant in univariate analysis were excluded. High miR-130b expression was found to be an independent prognostic factor of unfavorable DFS ($p = 0.013$; Table 4).

To further assess prognostic difference according to miR-130b expression, we used publicly available level 3 miRNA expression data and clinical information from TCGA. The mean follow-up period of the cohort was 29.3 months. Of the 435 cases, 154 showed tumor recurrence or progression and 153 died. There were no significant differences in DFS and OS between the high and low miRNA-130b expression groups ($p = 0.167$ and $p = 0.118$, respectively; Fig. 1c). In subgroup analyses according to tumor stage, high miRNA-130b expression was associated with shorter DFS in 243 stage I cases ($p = 0.006$; Fig. 1d). However, high miRNA-130b expression was not associated with OS ($p = 0.210$).

miR-130b regulates cell proliferation and migration in vitro

In NCI-H1650 cells, miR-130b expression was upregulated and downregulated using an miR-130b mimic and inhibitor, respectively, to investigate the functional role of miR-130b in the progression of lung adenocarcinoma. After transfection with miR-130b mimic and inhibitor, the expression of

Table 2 Correlation between microRNA-130b expression and various clinicopathologic parameters in lung adenocarcinoma.

Clinicopathologic parameters	microRNA-130b expression (dichotomized)				microRNA-130b expression (normalized using U6)	
	n	Low	High	*p* value[†]	Median	*p* value[‡]
Age						
<60 years	56	24 (42.9%)	32 (57.1%)	0.136	0.0056	0.138
≥60 years	90	50 (55.6%)	40 (44.4%)		0.0025	
Sex						
Male	63	30 (47.6%)	33 (52.4%)	0.506	0.0483	0.322
Female	83	44 (53.0%)	39 (47.0%)		0.0034	
Primary tumor size						
<3 cm	94	52 (55.3%)	42 (44.7%)	0.132	0.0028	0.190
≥3 cm	52	22 (42.3%)	30 (57.7%)		0.0054	
Histologic grade						
G1	27	23 (85.2%)	4 (14.8%)	<0.001	0.0016	0.002
G2, G3	119	51 (42.9%)	68 (57.1%)		0.0056	
Pathologic T category						
Tis, T1	66	41 (62.1%)	25 (37.9%)	0.012	0.0023	0.057
T2, T3, T4	80	33 (41.2%)	47 (58.8%)		0.0058	
AJCC stage						
I	90	54 (60.0%)	36 (40.0%)	0.004	0.0025	0.013
II, III, and IV	56	20 (35.7%)	36 (64.3%)		0.0081	
Lymph node metastasis						
Absent	104	59 (56.7%)	45 (43.3%)	0.021	0.0026	0.042
Present	42	15 (35.7%)	27 (64.3%)		0.0077	
Pleural invasion						
Absent	91	49 (53.8%)	42 (46.2%)	0.326	0.0034	0.883
Present	55	25 (45.5%)	30 (54.5%)		0.0043	
Lymphovascular invasion						
Absent	88	51 (58.0%)	37 (42.0%)	0.030	0.0022	0.052
Present	58	23 (39.7%)	35 (60.3%)		0.0059	
Perineural invasion						
Absent	117	58 (49.6%)	59 (50.4%)	0.589	0.0042	0.445
Present	29	16 (55.2%)	13 (44.8%)		0.0027	

AJCC American Joint Committee on Cancer.

[†]$\chi 2$ test; [‡]Mann–Whitney *U* test.

miR-130b assessed by qRT-PCR ($p < 0.001$, Fig. 2a). Cell proliferation was measured for 1 to 3 days using the MTT assay. Inhibited cell proliferation was detected in cells with downregulated miR-130b expression compared to negative control cells ($p < 0.05$; Fig. 2b).

Cell migration was investigated using the transwell migration and wound-healing assays. Compared with control cells, cells transfected with miR-130b inhibitor showed lesser migration ($p < 0.05$), while cells transfected with miR-130b mimic showed higher migration ($p < 0.05$) at 6 h after plating (Fig. 2c, d). Wound-healing assay indicated that cells with miR-130b upregulation and downregulation migrated to cover 60% and 14% of the initial wound area at 48 h after wounding, respectively. However, the control cells covered an average of 42% of the wound area (Fig. 2e, f). Moreover, the transwell invasion assay indicated that the number of invading cells was significantly increased after transfection with miR-130b mimic (Fig. 2g, h).

Discussion

The miR-130 family has been associated with the development of many cancers, probably via interfering with cellular processes, such as cell cycle, cell differentiation, epithelial–mesenchymal transition, and angiogenesis [21].

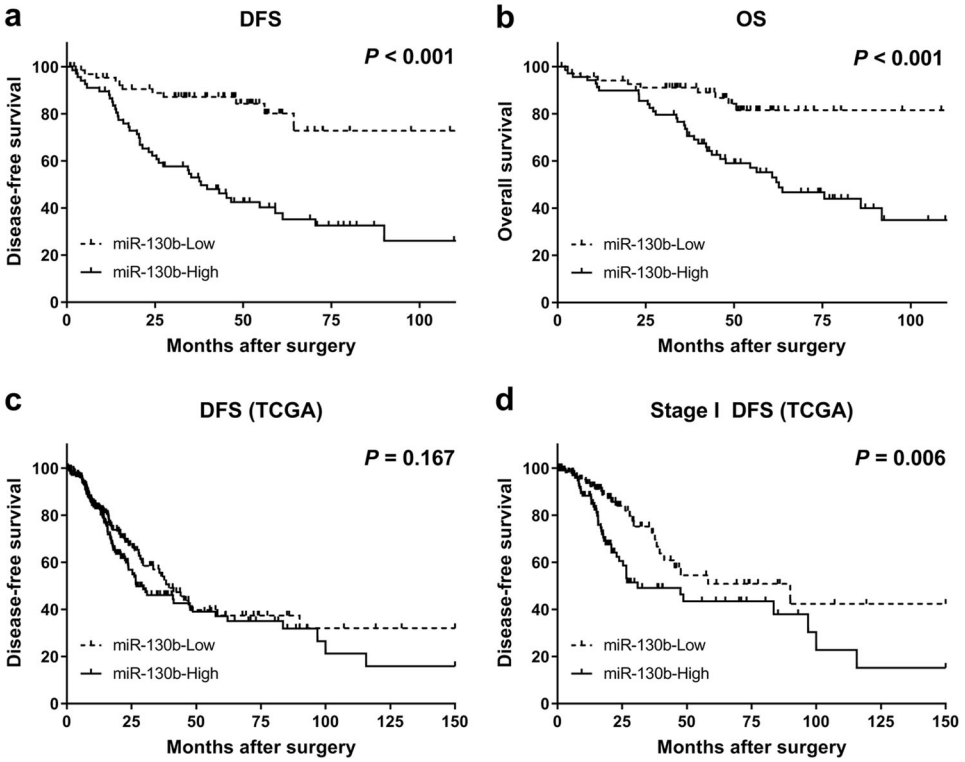

Fig. 1 Comparison of survival rates between low and high miR-130b expression groups. a Kaplan–Meier (KM) disease-free survival (DFS) curves for our cohort. **b** KM overall survival (OS) curves for our cohort. **c** KM DFS curves for lung adenocarcinoma using TCGA data ($n = 435$). **d** KM DFS curves for stage I lung adenocarcinoma using TCGA data ($n = 243$).

Table 3 Univariate Cox regression analysis of factors related to the prognosis of lung adenocarcinoma.

	Disease-free survival			Overall survival		
	HR	95% CI	*p* values	HR	95% CI	*p* values
Age (<60 years vs. ≥60 years)	1.072	0.623–1.847	0.801	1.602	0.864–2.968	0.135
Sex (male vs. female)	1.469	0.855–2.524	0.163	1.728	0.968–3.085	0.064
Primary tumor size (<3 cm vs. ≥3 cm)	2.175	1.268–3.729	0.005	2.183	1.223–3.895	0.008
Histologic grade (G1 vs. G2, G3)	5.010	1.560–16.089	0.007	5.364	1.299–22.150	0.020
Pathologic T category (Tis, T1 vs. T2, T3, T4)	2.052	1.166–3.612	0.013	2.355	1.265–4.384	0.007
AJCC stage (I vs. II, III, and IV)	4.560	2.596–8.009	<0.001	4.648	2.477–8.721	<0.001
Lymph node metastasis (absent vs. present)	3.188	1.858–5.472	<0.001	2.889	1.620–5.153	<0.001
Pleural invasion (absent vs. present)	1.145	0.643–2.039	0.647	2.154	1.186–3.911	0.012
Lymphovascular invasion (absent vs. present)	2.805	1.622–4.850	<0.001	2.700	1.483–4.914	0.001
Perineural invasion (absent vs. present)	2.123	1.175–3.835	0.013	1.830	0.959–3.495	0.067
MicroRNA-130b expression (low vs. high)	4.217	2.168–8.202	<0.001	3.267	1.618–6.598	0.001

AJCC American Joint Committee on Cancer, *HR* hazard ratio, *CI* confidence interval.

Previous studies have demonstrated the oncogenic role of miR-130b in glial tumor, bladder cancer, hepatocellular carcinoma (HCC), colorectal cancer, lung cancer, breast cancer, gastric cancer, and renal cell carcinoma [15, 19, 22, 23, 26–36]. Conversely, miR-130b has been shown to act as a tumor suppressor as well as an oncogene in breast, cervical, ovarian, gastric, prostatic, and pancreatic cancers and osteosarcoma [37–43].

In previous studies, miR-130b has been reported to cause various functional changes and induce tumorigenesis. miR-130b was shown to promotes migration and invasion in glioma [16, 28], esophageal cancer [17], bladder cancer [44], HCC [33], and Ewing sarcoma [18]. Moreover, miR-130b was shown to inhibit apoptosis in lung cancer [19], renal cell carcinoma [20], and glioma [27]. Several studies have shown that miR-130b contributes to angiogenesis in

Table 4 Multivariate Cox regression analysis of factors related to the prognosis of lung adenocarcinoma.

	Disease-free survival			Overall survival		
	HR	95% CI	*p* values	HR	95% CI	*p* values
Primary tumor size (<3 cm vs. ≥3 cm)	0.918	0.423–1.991	0.828	1.157	0.473–2.832	0.749
Histologic grade (G1 vs. G2, G3)	1.730	0.483–6.192	0.399	1.726	0.371–8.021	0.486
Pathologic T category (Tis, T1 vs. T2, T3, T4)	0.907	0.421–1.953	0.803	0.699	0.227–2.146	0.531
AJCC stage (I vs. II, III, and IV)	4.341	1.636–11.519	0.003	4.270	1.528–11.936	0.006
Lymph node metastasis (absent vs. present)	0.562	0.233–1.356	0.200	0.657	0.269–1.607	0.358
Pleural invasion (absent vs. present)				1.911	0.816–4.477	0.136
Lymphovascular invasion (absent vs. present)	1.674	0.879–3.190	0.117	1.520	0.769–3.005	0.229
Perineural invasion (absent vs. present)	1.415	0.739–2.709	0.295			
MicroRNA-130b expression (low vs. high)	0.013	1.214–5.208	0.013	1.927	0.916–4.054	0.084

AJCC American Joint Committee on Cancer, *HR* hazard ratio, *CI* confidence interval.

colorectal carcinoma [21] and chemoresistance in lung [23] and breast cancer [22]. In the present study, the oncogenic role of miR-130b was demonstrated using in vitro experiments. Our results demonstrated that the upregulation of miR-130b significantly promoted the migration and invasion of lung adenocarcinoma cells, whereas miR-130b downregulation inhibited cell proliferation and migration.

Previous studies using clinical data have shown that miR-130b overexpression is correlated with aggressive phenotypes and poor prognosis in various cancers, including glioma [16, 29, 45], HCC [33, 46], lung cancer [19], and bladder cancer [44]. Moreover, high miR-130b expression was associated with advanced WHO grade or TNM stage in all above-mentioned cancers, except colon cancer. In addition, poor histologic grade and high miR-130b expression were found to be correlated in all cancers, while distant metastasis and miR-130b expression levels were significantly correlated in colon and lung cancers [19, 21]. In HCC, venous invasion was significantly associated with alpha-fetoprotein level, HBsAg, and high miR-130b expression [33, 46]. Moreover, in previous studies on glioma [16, 45] and HCC [46], Kaplan–Meier analysis showed that miR-130b expression had a significant influence on OS, and high miR-130b expression was correlated with poor prognosis.

In the present study, high miR-130b expression was found to be significantly correlated with higher histologic grade, advanced pT stage, advanced AJCC stage, and lymph node metastasis. Furthermore, the DFS and OS of the high miR-130b expression group were significantly shorter than those of the low miR-130b expression group. In a multivariate Cox model, high miR-130b expression was found to be an independent poor prognostic factor of DFS. Therefore, our results support the notion that miR-130b might serve as a novel prognostic biomarker for lung adenocarcinoma. The survival curves from TCGA data are different from those of our cohort. According to the TCGA data, high miRNA-130b expression was associated with shorter DFS in only stage I cases. The patient outcome could be affected by several factors, such as follow-up period of cohort, patient's ethnicity, and method detecting miR-130b expression level. The ratio of each AJCC stage were similar with our cohort, however, the patient follow-up period of our cohort was much longer than that of TCGA data (mean follow-up period, 40.78 months vs. 20.93 months) and only Korean from single hospital was enrolled in our cohort. MiRNA expression level evaluated by next-generation sequencing technique for TCGA cohort and polymerase chain reaction for our cohort. Since this study only evaluated the miR-130b level in the patients with adenocarcinoma only, further studies with large cohort, including patients with other types of lung cancer, such as squamous cell carcinoma and small cell carcinoma, are needed.

Many studies indicated that miRNA can be a novel therapeutic target for human cancer. For miRNAs with oncogenic function, potential therapies include anti-miRNA oligonucleotides, miRNA sponges, miRNA masking, and small molecule inhibitor [47]. Several miRNA-targeted therapeutics have reached clinical development. The first miRNA-targeted therapy, MRX34 has started clinical trial for liver cancer in 2013 (NCT01829971) and miR-16-based therapy is currently under phase I clinical trials for patients with advanced non-small cell lung cancer (NCT02369198).

In conclusion, in this study, we highlighted the oncogenic role of miR-130b in lung adenocarcinoma and its significant correlation with adverse clinicopathologic parameters and poor patient outcome. Our data suggest that miR-130b may serve as a potential therapeutic target as well as a new prognostic biomarker of lung adenocarcinoma.

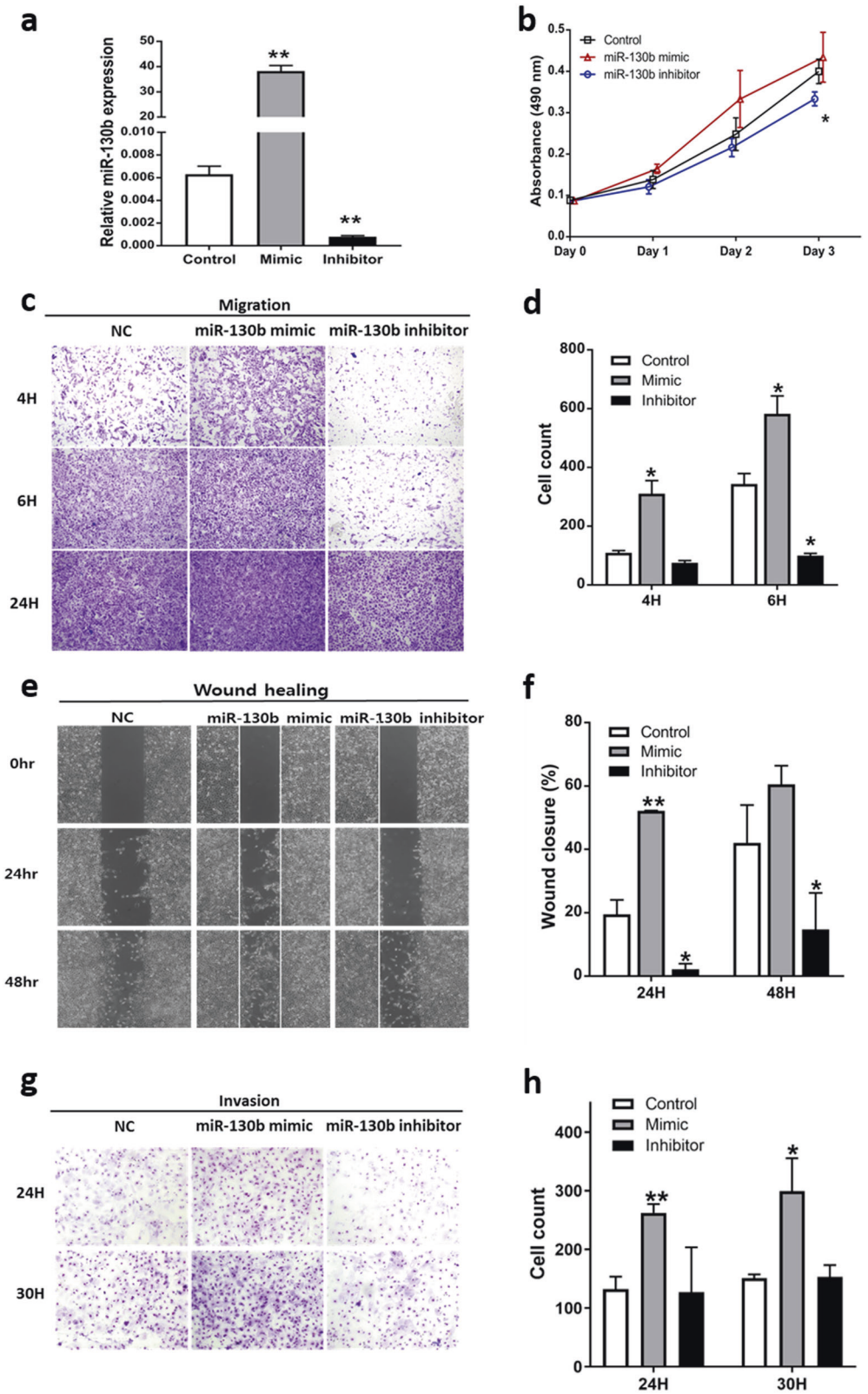

Fig. 2 In vitro effect of miR-130b on lung adenocarcinoma cell proliferation, migration, and invasion. a Expression level of miR-130b in NCI-H1650 cells. **b** Cell proliferation (MTT) assay. **c**, **d** Cell migration assay. **e**, **f** Wound-healing assay. **g**, **h** Invasion assay. (*$p < 0.05$, **$p < 0.01$).

Acknowledgements This research was supported by Basic Science Research Program through the National Research Foundation of Korea (NRF) funded by the Ministry of Education (NRF-2018R1D1A1B07048798). We would like to thank Sungwoong Kim, Jeongyun Eom, and Jisook Kim (Department of Pathology, Hanyang University Hospital) for their technical assistance.

Compliance with ethical standards

Conflict of interest The authors declare that they have no conflict of interest.

Publisher's note Springer Nature remains neutral with regard to jurisdictional claims in published maps and institutional affiliations.

References

1. Bray F, Ferlay J, Soerjomataram I, Siegel RL, Torre LA, Jemal A. Global cancer statistics 2018: GLOBOCAN estimates of incidence and mortality worldwide for 36 cancers in 185 countries. CA Cancer J Clin. 2018;68:394–424.
2. Duma N, Santana-Davila R, Molina JR. Non-small cell lung cancer: epidemiology, screening, diagnosis, and treatment. Mayo Clin Proc. 2019;94:1623–40.
3. Arbour KC, Riely GJ. Systemic therapy for locally advanced and metastatic non-small cell lung cancer: a review. JAMA. 2019;322:764–74.
4. Bartel DP. MicroRNAs: genomics, biogenesis, mechanism, and function. Cell. 2004;116:281–97.
5. Orellana EA, Kasinski AL. MicroRNAs in cancer: a historical perspective on the path from discovery to therapy. Cancers. 2015;7:1388–405.
6. Calin GA, Croce CM. MicroRNA signatures in human cancers. Nat Rev Cancer. 2006;6:857–66.
7. Kobayashi H, Tomari Y. RISC assembly: coordination between small RNAs and argonaute proteins. Biochim Biophys Acta. 2016;1859:71–81.
8. Wen D, Danquah M, Chaudhary AK, Mahato RI. Small molecules targeting microRNA for cancer therapy: promises and obstacles. J Control Release. 2015;219:237–47.
9. Li J, Yang J, Zhou P, Le Y, Zhou C, Wang S, et al. Circular RNAs in cancer: novel insights into origins, properties, functions and implications. Am J Cancer Res. 2015;5:472–80.
10. Zaravinos A. The regulatory role of microRNAs in EMT and cancer. J Oncol. 2015;2015:865816.
11. Lan H, Lu H, Wang X, Jin H. MicroRNAs as potential biomarkers in cancer: opportunities and challenges. Biomed Res Int. 2015;2015:125094.
12. Osaki M, Okada F, Ochiya T. miRNA therapy targeting cancer stem cells: a new paradigm for cancer treatment and prevention of tumor recurrence. Ther Deliv. 2015;6:323–37.
13. Lu J, Getz G, Miska EA, Alvarez-Saavedra E, Lamb J, Peck D, et al. MicroRNA expression profiles classify human cancers. Nature. 2005;435:834–8.
14. Di Leva G, Croce CM. miRNA profiling of cancer. Curr Opin Genet Dev. 2013;23:3–11.
15. Egawa H, Jingushi K, Hirono T, Ueda Y, Kitae K, Nakata W, et al. The miR-130 family promotes cell migration and invasion in bladder cancer through FAK and Akt phosphorylation by regulating PTEN. Sci Rep. 2016;6:20574.
16. Sheng X, Chen H, Wang H, Ding Z, Xu G, Zhang J, et al. MicroRNA-130b promotes cell migration and invasion by targeting peroxisome proliferator-activated receptor gamma in human glioma. Biomed Pharmacother. 2015;76:121–6.
17. Yu T, Cao R, Li S, Fu M, Ren L, Chen W, et al. MiR-130b plays an oncogenic role by repressing PTEN expression in esophageal squamous cell carcinoma cells. BMC Cancer. 2015;15:29.
18. Satterfield L, Shuck R, Kurenbekova L, Allen-Rhoades W, Edwards D, Huang S, et al. miR-130b directly targets ARHGAP1 to drive activation of a metastatic CDC42-PAK1-AP1 positive feedback loop in Ewing sarcoma. Int J Cancer. 2017;141:2062–75.
19. Tian J, Hu L, Li X, Geng J, Dai M, Bai X. MicroRNA-130b promotes lung cancer progression via PPARgamma/VEGF-A/BCL-2-mediated suppression of apoptosis. J Exp Clin Cancer Res. 2016;35:105.
20. Li Y, Chen D, Li Y, Jin L, Liu J, Su Z, et al. Identification of miR130b as an oncogene in renal cell carcinoma. Mol Med Rep. 2016;13:1902–8.
21. Colangelo T, Fucci A, Votino C, Sabatino L, Pancione M, Laudanna C, et al. MicroRNA-130b promotes tumor development and is associated with poor prognosis in colorectal cancer. Neoplasia. 2013;15:1086–99.
22. Miao Y, Zheng W, Li N, Su Z, Zhao L, Zhou H, et al. MicroRNA-130b targets PTEN to mediate drug resistance and proliferation of breast cancer cells via the PI3K/Akt signaling pathway. Sci Rep. 2017;7:41942.
23. Zhang Q, Zhang B, Sun L, Yan Q, Zhang Y, Zhang Z, et al. MicroRNA-130b targets PTEN to induce resistance to cisplatin in lung cancer cells by activating Wnt/beta-catenin pathway. Cell Biochem Funct. 2018;36:194–202.
24. Travis WD, Brambilla E, Burke AP, Marx A, Nicholson AG. Introduction to the 2015 world health organization classification of tumors of the lung, pleura, thymus, and heart. J Thorac Oncol. 2015;10:1240–2.
25. Goldstraw P, Chansky K, Crowley J, Rami-Porta R, Asamura H, Eberhardt WE, et al. The IASLC lung cancer staging project: proposals for revision of the TNM stage groupings in the forthcoming (eighth) edition of the TNM classification for lung cancer. J Thorac Oncol. 2016;11:39–51.
26. Liu X, Kong C, Zhang Z. miR-130b promotes bladder cancer cell proliferation, migration and invasion by targeting VGLL4. Oncol Rep. 2018;39:2324–32.
27. Gu JJ, Fan KC, Zhang JH, Chen HJ, Wang SS. Suppression of microRNA-130b inhibits glioma cell proliferation and invasion, and induces apoptosis by PTEN/AKT signaling. Int J Mol Med. 2018;41:284–92.
28. Gu JJ, Zhang JH, Chen HJ, Wang SS. MicroRNA-130b promotes cell proliferation and invasion by inhibiting peroxisome proliferator-activated receptor-gamma in human glioma cells. Int J Mol Med. 2016;37:1587–93.
29. Li B, Liu YH, Sun AG, Huan LC, Li HD, Liu DM. MiR-130b functions as a tumor promoter in glioma via regulation of ERK/MAPK pathway. Eur Rev Med Pharmacol Sci. 2017;21:2840–6.
30. Xiao ZQ, Yin TK, Li YX, Zhang JH, Gu JJ. miR-130b regulates the proliferation, invasion and apoptosis of glioma cells via targeting of CYLD. Oncol Rep. 2017;38:167–74.
31. Lv M, Zhong Z, Chi H, Huang M, Jiang R, Chen J. Genome-wide screen of miRNAs and targeting mRNAs reveals the negatively regulatory effect of miR-130b-3p on PTEN by PI3K and integrin beta1 signaling pathways in bladder carcinoma. Int J Mol Sci. 2016;18:78.
32. Hu XY, Li L, Wu HT, Liu Y, Wang BD, Tang Y. Serum miR-130b level, an ideal marker for monitoring the recurrence and prognosis of primary hepatocellular carcinoma after radiofrequency ablation treatment. Pathol Res Pract. 2018;214:1655–60.
33. Tu K, Zheng X, Dou C, Li C, Yang W, Yao Y, et al. MicroRNA-130b promotes cell aggressiveness by inhibiting peroxisome

proliferator-activated receptor gamma in human hepatocellular carcinoma. Int J Mol Sci. 2014;15:20486–99.
34. Yi R, Li Y, Wang F, Gu J, Isaji T, Li J, et al. Transforming growth factor (TGF) beta1 acted through miR-130b to increase integrin alpha5 to promote migration of colorectal cancer cells. Tumour Biol. 2016;37:10763–73.
35. Chen H, Yang Y, Wang J, Shen D, Zhao J, Yu Q. miR-130b-5p promotes proliferation, migration and invasion of gastric cancer cells via targeting RASAL1. Oncol Lett. 2018;15:6361–7.
36. Lai KW, Koh KX, Loh M, Tada K, Subramaniam MM, Lim XY, et al. MicroRNA-130b regulates the tumour suppressor RUNX3 in gastric cancer. Eur J Cancer. 2010;46:1456–63.
37. Shui Y, Yu X, Duan R, Bao Q, Wu J, Yuan H, et al. miR-130b-3p inhibits cell invasion and migration by targeting the Notch ligand Delta-like 1 in breast carcinoma. Gene. 2017;609:80–87.
38. Paudel D, Zhou W, Ouyang Y, Dong S, Huang Q, Giri R, et al. MicroRNA-130b functions as a tumor suppressor by regulating RUNX3 in epithelial ovarian cancer. Gene. 2016;586:48–55.
39. Sun B, Li L, Ma W, Wang S, Huang C. MiR-130b inhibits proliferation and induces apoptosis of gastric cancer cells via CYLD. Tumour Biol. 2016;37:7981–7.
40. Chen Q, Zhao X, Zhang H, Yuan H, Zhu M, Sun Q, et al. MiR-130b suppresses prostate cancer metastasis through down-regulation of MMP2. Mol Carcinog. 2015;54:1292–1300.
41. Zhao G, Zhang JG, Shi Y, Qin Q, Liu Y, Wang B, et al. MiR-130b is a prognostic marker and inhibits cell proliferation and invasion in pancreatic cancer through targeting STAT3. PLoS One. 2013;8:e73803.
42. Wu Y, Sun W, Kong Y, Liu B, Zeng M, Wang W. Restoration of microRNA-130b expression suppresses osteosarcoma cell malignant behavior in vitro. Oncol Lett. 2018;16:97–104.
43. Yang L, Wang Y, Shi S, Xie L, Liu T, Wang Y, et al. The TNF-alpha-induced expression of miR-130b protects cervical cancer cells from the cytotoxicity of TNF-alpha. FEBS Open Bio. 2018;8:614–27.
44. Cui X, Kong C, Zhu Y, Zeng Y, Zhang Z, Liu X, et al. miR-130b, an onco-miRNA in bladder cancer, is directly regulated by NF-kappaB and sustains NF-kappaB activation by decreasing Cylindromatosis expression. Oncotarget. 2016;7:48547–61.
45. Li P, Wang X, Shan Q, Wu Y, Wang Z. MicroRNA-130b promotes cell migration and invasion by inhibiting peroxisome proliferator-activated receptor-gamma in human glioma. Oncol Lett. 2017;13:2615–22.
46. Wang WY, Zhang HF, Wang L, Ma YP, Gao F, Zhang SJ, et al. High expression of microRNA-130b correlates with poor prognosis of patients with hepatocellular carcinoma. Diagn Pathol. 2014;9:160.
47. Li C, Feng Y, Coukos G, Zhang L. Therapeutic microRNA strategies in human cancer. AAPS J. 2009;2009:747–757.